Activity level controls postsynaptic composition and signaling via the ubiquitin-proteasome system

Michael D. Ehlers[1]

[1] *Department of Neurobiology, Box 3209, Duke University Medical Center, Durham, North Carolina 27710, USA*
Correspondence should be addressed to M.D.E. (ehlers@neuro.duke.edu)

Published online 10 February 2003; doi:10.1038/nn1013

Experience-dependent remodeling of the postsynaptic density (PSD) is critical for synapse formation and plasticity in the mammalian brain. Here, in cultured rat hippocampal neurons, I found long-lasting, global changes in the molecular composition of the PSD dictated by synaptic activity. These changes were bidirectional, reversible, modular, and involved multiple classes of PSD proteins. Moreover, activity-dependent remodeling was accompanied by altered protein turnover, occurred with corresponding increases or decreases in ubiquitin conjugation of synaptic proteins and required proteasome-mediated degradation. These modifications, in turn, reciprocally altered synaptic signaling to the downstream effectors CREB (cyclic AMP response element binding protein) and ERK-MAPK (extracellular signal regulated kinase–MAP kinase). These results indicate that activity regulates postsynaptic composition and signaling through the ubiquitin-proteasome system, providing a mechanistic link between synaptic activity, protein turnover and the functional reorganization of synapses.

© 2003 Nature Publishing Group http://www.nature.com/natureneuroscience

The remodeling of synapses is a fundamental mechanism for information storage and processing in the brain[1,2]. Much of this remodeling occurs at the postsynaptic density (PSD), a specialized biochemical apparatus containing glutamate receptors and associated scaffolding proteins that organize signal transduction pathways at the postsynaptic membrane[3,4]. During synapse maturation and in response to synaptic activity, the PSD undergoes remarkable structural changes[2], including growth[5], complexification and perforation[6,7] and dynamic turnover[8,9]. Such structural plasticity is thought to be accompanied and mediated by changes in the molecular composition and signaling properties of the PSD[2,4]. Indeed, stabilization or removal of glutamate receptors and signaling proteins from the PSD has been proposed to account for long-term changes in synaptic strength occurring over time frames ranging from minutes to days[2,10–15]. Nevertheless, with few exceptions, the specific (and likely numerous) molecular changes that occur in the PSD in response to synaptic activity remain unknown.

Long-lasting changes in the molecular content of synapses could arise by the incorporation of new proteins or by the selective stabilization or removal of existing synaptic proteins. Currently, the prevailing model for enduring changes in synapse function and structure is stimulus-dependent gene expression and protein synthesis[16,17]. Indeed, substantial evidence indicates that transcriptional events are critical for long-term, activity-dependent plasticity[16,18]. In addition, several studies support a role for local translation of dendritic mRNAs in orchestrating long-lasting forms of learning-related synaptic plasticity[17]. Compared to gene transcription and protein synthesis, considerably less attention has been placed on the contribution of protein turnover to long-term structural and functional changes at synapses.

One of the major cellular mechanisms controlling protein turnover is covalent attachment of ubiquitin and subsequent degradation by the proteasome[19]. In response to various stimuli, ubiquitin—a highly conserved, 76 amino acid polypeptide—is covalently linked to lysine residues of proteins by the sequential action of ubiquitin-activating enzymes (E1), ubiquitin-conjugating enzymes (E2) and ubiquitin ligases (E3)[19]. The addition of single ubiquitin moieties influences protein trafficking between cellular compartments[20]. The addition of multiple ubiquitin in chains targets proteins for degradation by the multi-subunit proteasome complex[19]. Regulated protein degradation by the ubiquitin-proteasome system is crucial for many cellular functions, including cell-cycle control, cell fate and growth, antigen presentation and cell signaling[19]. More recently, ubiquitin-processing enzymes have been found to regulate synapse growth and development, synaptic transmission, and plasticity at both invertebrate and mammalian synapses[21–25], suggesting a potential role for ubiquitin-dependent mechanisms in organizing synaptic structures and signaling complexes[25,26]. Indeed, at *C. elegans* sensory interneuron synapses, postsynaptic glutamate receptors themselves can be ubiquitinated, a process that decreases their abundance at the synapse[27]. Intriguingly, ubiquitinated proteins are abundant in the postsynaptic density of mammalian synapses[28], yet the identity of these proteins, the regulation of their ubiquitination, and the molecular and functional consequences of these modifications remain unknown.

In this study, I investigated the global compositional changes that occur in the PSD in response to altered synaptic activity

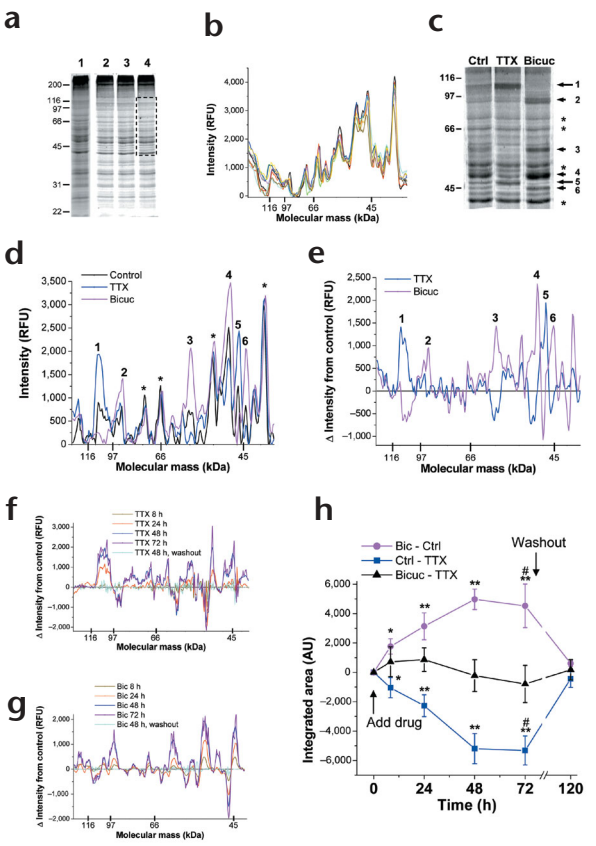

Fig. 1. Synaptic activity bidirectionally and reversibly regulates the composition of the PSD. (**a**) Total protein stains of PSD fractions isolated from rat brain (lane 1) and cultured cortical neurons (lanes 2–4). Molecular mass markers in kDa are shown. Equal protein amounts (1–2 μg) were loaded in all cases. (**b**) Linescan analysis of total protein revealed marked similarity between PSD fractions from two rat brains and six cortical neuron cultures. The proteins analyzed encompass the boxed region in (**a**). (**c**) The pattern of proteins present in the PSD changes in response to both synaptic blockade (TTX, 2 μM, 48 h) and excitatory synaptic activation (Bicuc, 40 μM, 48 h). Protein bands that increased in intensity with TTX (long arrows) or bicuculline (short arrows), or remained unchanged (asterisks), are indicated. (**d**) Overlaid line scans of total PSD protein from control, TTX-treated and bicuculline-treated cortical neurons. Numbered and asterisked peaks correspond to bands indicated in (**c**). (**e**) Absolute changes in protein signal intensity in PSD fractions from synaptically active (Bicuc, 40 μM, 48 h) and synaptically inhibited (TTX, 2 μM, 48 h) cortical neurons relative to control. Numbered peaks correspond to arrows in (**c**). (**f**) Absolute changes in protein signal intensity in PSD fractions from cortical neurons treated for various times with TTX (2 μM; 8, 24, 48 or 72 h as indicated) or cortical neurons treated for 48 h with TTX followed by washout for 48 h relative to control. (**g**) Absolute changes in protein signal intensity in PSD fractions over time from synaptically active (Bic, 40 μM) cortical neurons relative to control. (**h**) Quantitative analysis of activity-dependent changes in PSD protein profiles. Data represent means ± s.e.m. of integrated areas expressed in arbitrary units (AU) derived from the absolute values of subtracted protein signal intensity curves in (**f**) and (**g**) (*P < 0.01, **P < 0.001 relative to zero change; t-test, n = 6). Note that this parameter of deviation away from control plateaus between 48 and 72 h (#, P > 0.1 relative to 48 h time point, t-test) and reverses after drug washout.

and the regulation of such changes by ubiquitin-dependent protein turnover. Using quantitative protein expression profiling, I show that activity bidirectionally and reversibly regulates PSD composition. This reorganization involves glutamate receptors, scaffolds/adaptors and signaling enzymes that behave as coregulated protein ensembles. Activity-level controls protein stability and half-life in the PSD and regulates ubiquitin conjugation of postsynaptic proteins. Furthermore, activity-dependent changes in PSD composition require ubiquitin-proteasome–mediated degradation, and these molecular modifications alternately augment or suppress synaptic signaling via CREB and ERK-MAPK. These results identify activity-dependent protein turnover as a new mechanism controlling synapse remodeling and signaling. The present findings also support the idea that both the molecular and functional plasticity of synapses rely on a dynamic balance between synaptic activity and ubiquitin-dependent removal of synaptic proteins.

Results

PSD composition at active and inactive synapses

To examine activity-dependent changes in the PSD, I used a quantitative protein profiling approach, which includes a modified procedure for isolating PSDs from cultured cortical neurons[29] along with one-dimensional protein profile linescan analysis. The protein intensity profiles of PSD fractions isolated from cortical neurons were highly reproducible and nearly identical to those from rat forebrain PSDs (**Fig. 1a** and **b**). Blocking action potential–dependent synaptic activity with the Na^+ channel blocker tetrodotoxin (TTX, 2 μM, 48 h), or increasing excitatory synaptic activity by blocking inhibitory GABAergic transmission with the $GABA_A$ receptor antagonist bicuculline (40 μM, 48 h), had profound effects on the protein expression pattern in the PSD (**Fig. 1c**). In fact, these two well-characterized pharmacological treatments[8,30,31] elicited reciprocal changes. That is, protein bands whose intensity increased in TTX tended to decrease in bicuculline and vice-versa (**Fig. 1c–e**; also see **Fig. 2**). This effect of activity required postsynaptic glutamate receptor activation, as the addition of CNQX (10 μM) plus D-AP5 (50 μM)—selective antagonists for AMPA and NMDA-type glutamate receptors, respectively—resulted in PSD protein intensity profiles that were indistinguishable from those of TTX-treated neurons (data not shown).

To determine the kinetics of protein profile changes at active and inactive synapses, PSDs were isolated from cortical neurons at various times after adding TTX or bicuculline. Total protein visualization and one-dimensional linescan analysis showed small deviations from control after 8 hours of altered synaptic activity, which steadily increased in magnitude over the subsequent 16–40 hours, plateaued and remained stable after 48 hours, and returned to control patterns after drug washout (**Fig. 1f** and **g**). As a quantitative measure of net difference between protein profiles, absolute values of subtracted intensity curves were obtained, and the integrated area under the curves was measured. This analysis showed that activity-dependent changes in PSD composition occurred slowly, reached steady state after 48 hours (P > 0.1 between 48 and 72 h time points, t-test) and reversed completely upon drug washout (**Fig. 1h**). In addition, subtracting protein intensity curves of inhibited PSDs from synaptically active PSDs (Bicuc minus TTX) gave near-zero values at all time points (**Fig. 1h**), indicating the reciprocal nature of activity-dependent changes.

© 2003 Nature Publishing Group http://www.nature.com/natureneuroscience

© 2003 Nature Publishing Group http://www.nature.com/natureneuroscience

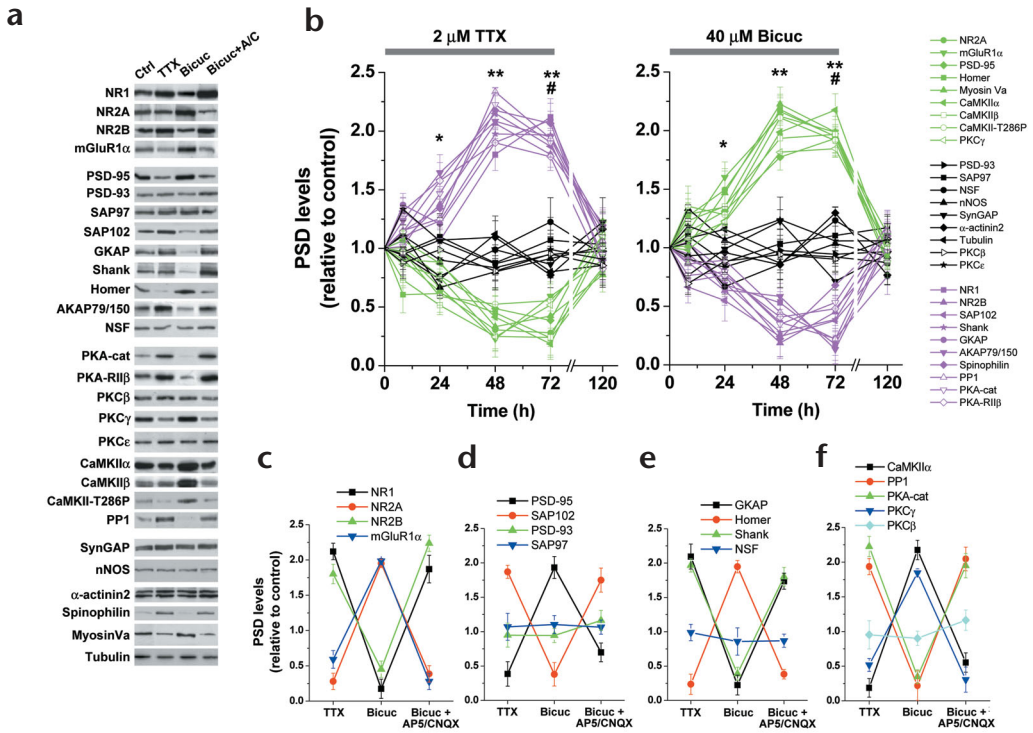

Fig. 2. Postsynaptic protein ensembles coregulated by activity. (**a**) Immunoblot analysis of selected proteins in PSD fractions isolated from cortical neurons treated for 48 h with control solution (Ctrl), TTX (2 μM), bicuculline (Bicuc, 40 μM) or bicuculline plus 50 μM D-AP5 and 10 μM CNQX (Bicuc + A/C). (**b**) Quantitative analysis of selected PSD proteins at various times after adding and then removing TTX (left) or bicuculline (right). The gray bars indicate duration of drug treatment. Data represent means ± s.e.m. of band intensities normalized to control values from untreated control neuron PSDs (*$P < 0.05$ for all pairwise comparisons between red and green proteins; **$P < 0.01$ for all pairwise comparisons between red, green and black proteins; *t*-test; $n = 3$–6 for each time point). Note that in almost all cases, net change in protein levels from control values reached steady state between 48 and 72 h (#, $P > 0.05$ relative to 48 h time point, *t*-test; see also **Supplementary Table 1**). (**c**–**f**) The abundance of selected glutamate receptors (**c**), MAGUK proteins (**d**), other scaffolding/trafficking proteins (**e**) and protein kinases/phosphatases (**f**) in PSDs isolated from cortical neurons treated with TTX, bicuculline or bicuculline plus D-AP5 and CNQX. Data represent means ± s.e.m. of band intensities 72 h after drug treatment, normalized to control values from untreated control neuron PSDs. Note that abscissa values reflect drug treatments, not time.

Together, these findings provide direct evidence that the overall molecular organization of the PSD is determined by the level of excitatory synaptic activity.

Coregulated 'clusters' of PSD proteins

To identify specific proteins that account for the global change in PSD composition, I carried out quantitative immunoblot analysis on synaptically active and synaptically inhibited PSD fractions using a panel of 28 different antibodies against neurotransmitter receptors, scaffold proteins and signaling molecules (**Fig. 2a**). This analysis allowed a classification of PSD proteins into three distinct categories: those whose relative abundance increased, decreased or remained unchanged when synaptic activity was decreased with TTX (**Fig. 2b,** left panel). Remarkably, the behavior of these proteins was exactly the opposite when excitatory synaptic activity was increased with bicuculline (**Fig. 2b**, right panel). Specifically, all proteins whose abundance increased with TTX blockade decreased in synaptically active (bicuculline-treated) PSDs, and all proteins that decreased with synaptic blockade increased upon synaptic activation (**Fig. 2b**; see also **Supplementary Table 1** online). Proteins unaffected by synaptic blockade were likewise unaffected by synaptic activation (**Fig. 2b**). As with changes in the one-dimensional protein profiles (**Fig. 1**), the changes in PSD levels of examined proteins were slow, reversible, and in nearly all cases, reached steady-state by 48 –72 hours (**Fig. 2b** and **Supplementary Table 1**). Moreover, for all proteins examined, glutamate receptor blockade (50 μM D-AP5, 10 μM CNQX) mimicked the effect of TTX even in the presence of bicuculline (**Fig. 2a** and data not shown). Importantly, the abundance of tubulin, a well-known 'contaminant' of the PSD prep, was unchanged by the pharmacological treatments (**Fig. 2a** and **b**; **Supplementary Table 1**), indicating the specificity of the drugs and the similarity in PSD preps under the various conditions. Likewise, activity manipulation of these mature cultures had no detectable effect on neuronal growth, density or survival (data not shown).

An interesting feature of the observed increases or decreases in protein abundance was that several PSD proteins within specific protein classes showed reciprocal activity-dependent behavior (**Fig. 2b** and **Supplementary Table 1**). For example, the NMDA receptor subunit NR2A accumulated in active PSDs, whereas the NR2B subunit prevailed at inactive synapses (**Fig. 2c**). Likewise, PSD-95, a major scaffolding protein at excitatory synapses, was enriched in PSDs from synaptically active neurons and reduced in PSD fractions from synaptically inhibited neurons, a pattern exactly opposite that of the related protein SAP102 (**Fig. 2d**). Similarly, the multivalent scaffold proteins Shank and GKAP accrued at inactive synapses, whereas Homer, an adaptor protein frequently associated with Shank and GKAP[32], was plentiful at active synapses (**Fig. 2e**). Furthermore, the abundant signaling enzymes Ca^{2+}/calmodulin-dependent protein kinase type II (CaMKII)

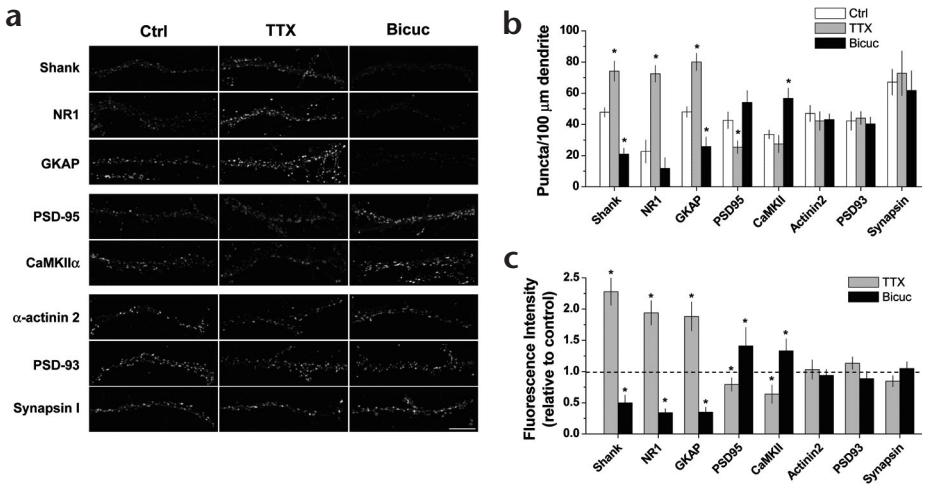

Fig. 3. Activity-dependent accumulation or reduction of PSD proteins at synaptic sites. (**a**) Cultured hippocampal neurons (24–30 days *in vitro*, d.i.v.) were treated with either 2 μM TTX, 40 μM bicuculline (Bicuc), or control solution for 48 h before fixation, permeabilization and staining for synaptic proteins. Scale bar, 10 μm. (**b**, **c**) Quantitative analysis showed changes in the number of PSD protein puncta per 100-μm dendrite (**b**) and in synaptic fluorescence intensity (**c**) consistent with the biochemical data of **Fig. 2**. Note that the overall number of synapses revealed by synapsin staining was unchanged. Data represent means ± s.e.m. from 20 neurons for each condition. *$P < 0.01$ relative to control, *t*-test.

and protein phosphatase 1 (PP1), as well as protein kinase C (PKC) and protein kinase A (PKA), showed mirror image patterns of PSD accumulation in TTX- and bicuculline-treated neurons (**Fig. 2f**). Together, these experiments show that changes in multiple classes of proteins account for activity-dependent PSD reorganization and indicate that distinct 'clusters' of postsynaptic proteins are coregulated by activity.

To determine whether the observed changes in PSD protein levels occurred globally or were restricted to a subset of excitatory synapses or a subpopulation of neurons, immunofluorescent staining was performed on hippocampal neurons after 48 hours of synaptic blockade (2 μM TTX) or synaptic activation (40 μM bicuculline) (**Fig. 3a**). Treatment with TTX resulted in a marked increase in both the number and staining intensity of Shank, NR1 and GKAP immunoreactive clusters (**Fig. 3b** and **c**). In contrast, staining for PSD-95 and CaMKIIα was slightly decreased by prolonged synaptic blockade (**Fig. 3b** and **c**), whereas no quantitative changes were observed in staining for α-actinin2 or PSD-93 (**Fig. 3b** and **c**). Precisely the opposite pattern of changes was observed in highly active cultures (**Fig. 3a**, right panels), namely a robust decrease in the number and intensity of Shank, NR1 and GKAP puncta and a small increase in PSD-95 and CaMKIIα staining (**Fig. 3b** and **c**). In all cases, the punctate clusters of PSD proteins colocalized with synapsin I (data not shown), indicating localization opposite presynaptic terminals. Moreover, observed changes in synaptic staining occurred over all neurons examined ($n = 20$ for each condition), with no observable differences between synapses on individual neurons (**Fig. 3a** and data not shown). In addition, treatment with TTX or bicuculline had no effect on the number or staining intensity of synapsin puncta (**Fig. 3b** and **c**), indicating that chronic changes in synaptic activity did not alter the number of synapses, consistent with previous studies[12,13,33]. These results support the biochemical data obtained in **Fig. 2** and extend previous work[12,13,34] by showing that chronic sustained alterations in activity produce global bidirectional changes in multiple postsynaptic molecules.

Activity controls global protein turnover in the PSD

Activity-dependent changes in PSD composition could arise by incorporation of new proteins or by regulated removal/loss of synaptic proteins. A suggested mechanism for activity-dependent synapse remodeling is the dynamic turnover of the PSD itself[8,9]. Thus, the effect of activity on the stabilization and/or loss of PSD proteins was examined. Specifically, the half-life or turnover rate of synaptic proteins in PSD fractions and synaptosomes was measured using ^{35}S-cysteine/methionine metabolic labeling pulse-chase analysis. This method provides a direct measure of the rate

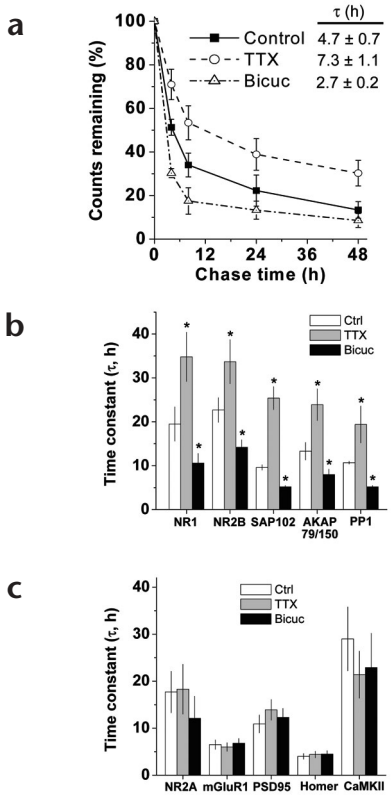

Fig. 4. Activity level controls protein half-life in synaptic fractions. (**a**) Loss of total ^{35}S-labeled protein from control, TTX- and bicuculline-treated cortical neuron PSDs at various times after a 12 h pulse (± s.e.m., $n = 6$). (**b**, **c**) Quantification of the effect of decreased (TTX) and increased (Bicuc) synaptic activity on the rate of loss of selected PSD proteins isolated by immunoprecipitation from synaptosomes taken from ^{35}S-labeled control, TTX- and bicuculline-treated cortical neurons at various times after a 12 h pulse (± s.e.m., $n = 6$). Time constants are derived from single exponential fits of turnover time course data. (*$P < 0.01$, *t*-test, $n = 4$–6).

© 2003 Nature Publishing Group http://www.nature.com/natureneuroscience

© 2003 Nature Publishing Group http://www.nature.com/natureneuroscience

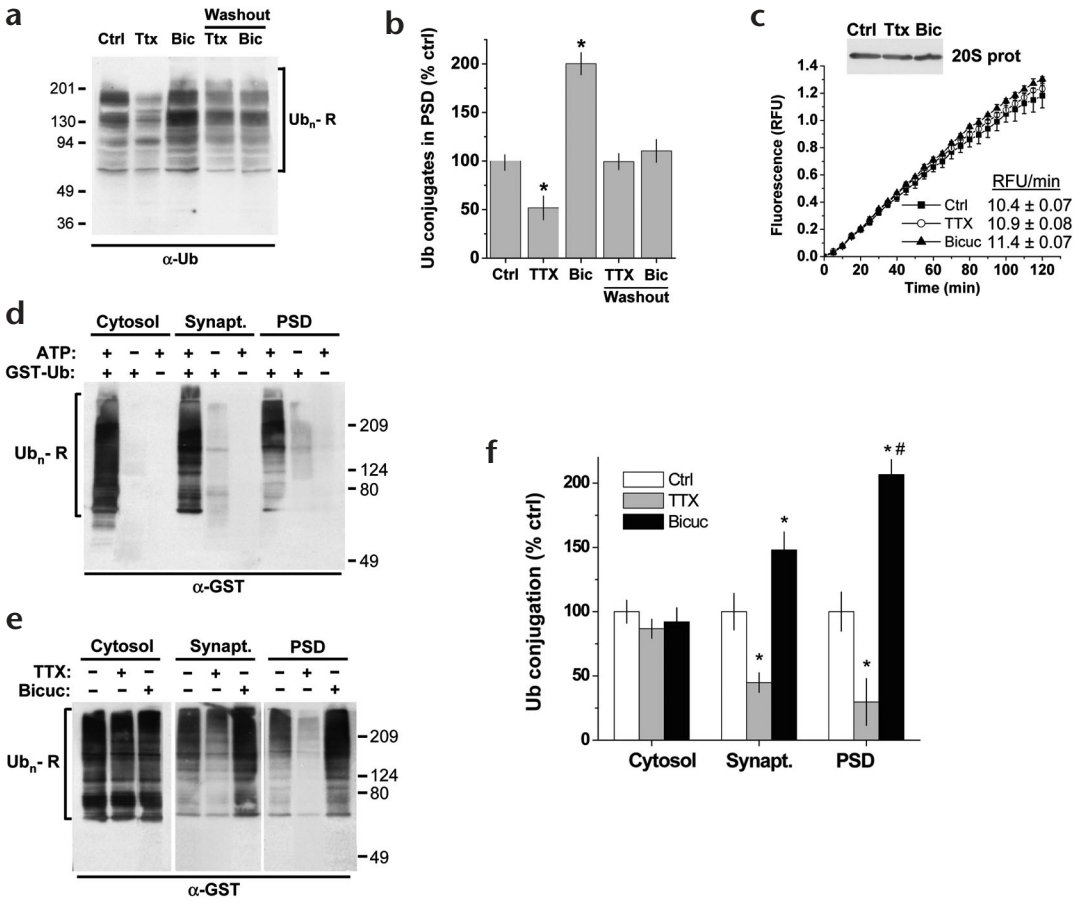

Fig. 5. Synaptic activity increases ubiquitin conjugation of PSD proteins. (**a**) Immunoblot analysis of ubiquitin (Ub) conjugates in PSD fractions isolated from control (Ctrl), TTX-treated (TTX, 2 μM, 48 h) or bicuculline-treated (Bic, 40 μM, 48 h) cortical neurons immediately after drug treatment (lanes 1–3) or 48 more hours after a subsequent drug washout (lanes 4 and 5). Molecular mass markers in kDa are shown. (**b**) Quantitative analysis of the effects of TTX and bicuculline (Bic) on ubiquitin conjugate abundance in the PSD. (*P < 0.01, n = 6, t-test). (**c**) Proteasome activity assays and immunoblot analysis of 20S proteasome (inset) in control (Ctrl), TTX-treated (TTX) or bicuculline-treated (Bic) cortical neurons revealed no effect of activity on proteasome activity or expression levels. Proteasome activity in RFU/min is shown (± s.e.m., n = 8). (**d**) *De novo* ubiquitin conjugation of synaptic proteins. Ubiquitin conjugation assays on rat brain cytosol or synaptosomes (Synapt.) were conducted in the presence (+) or absence (–) of ATP and GST-ubiquitin (GST-Ub). Samples were either immediately solubilized, or PSD fractions were purified. Newly formed ubiquitin-conjugates (Ub$_n$-R) were detected by immunoblot analysis with α-GST antibody. (**e**) *De novo* ubiquitin conjugation in cytosol, synaptosome and PSD fractions isolated from control, synaptically inhibited (+TTX, –Bicuc) and synaptically activated (–TTX, +Bicuc) cortical neurons. (**f**) Quantitative analysis of the effect of increased (Bicuc) and decreased (TTX) activity on ubiquitin conjugation in cortical neuron fractions. (*P < 0.001 relative to control; #, P < 0.01 relative to bicuculline-treated synaptosomes; n = 6, t-test).

of permanent loss (turnover) of proteins from the examined pool (for example, PSD or synaptosomes). Such turnover reflects a combination of loss by degradation and loss by permanent transport out of the synaptic pool.

Pulse-chase analysis revealed surprisingly robust ongoing turnover of total PSD protein in control neurons ($\tau = 4.7 \pm 0.7$ h) that was accelerated by excitatory synaptic activity (40 μM bicuculline; $\tau = 2.7 \pm 0.2$ h) and slowed in inactive cultures (2 μM TTX; $\tau = 7.3 \pm 1.1$ h) (**Fig. 4a**). The activity-dependent increase in total PSD protein turnover was mirrored by an increase in the rate of loss of a subset of PSD proteins from cortical neuron synaptosomes. Turnover rates for ten proteins reflecting receptors (NR1, NR2A, NR2B, mGluR1), scaffold/adaptor proteins (PSD-95, SAP102, AKAP79/150, Homer) and signaling enzymes (CaMKII, PP1) whose abundance in the PSD was regulated by activity (**Fig. 2**) were selected for analysis by ^{35}S pulse-chase and immunoprecipitation from synaptosomes. Of these, five proteins (NR1, NR2B, SAP102, AKAP79/150 and PP1) showed turnover rates that increased or decreased in parallel with the level of synaptic activity (**Fig. 4b**). In contrast, the turnover of five related proteins (NR2A, mGluR1, PSD-95, Homer and CaMKII) was unaffected by changes in synaptic activity (**Fig. 4c**). It is important to note that the rate of loss of a protein from synaptosomes (**Fig. 4b** and **c**) may differ from the half-life in the PSD fraction (**Fig. 4a**) because the PSD represents only a subset of the synaptosome fraction. Nonetheless, the rates measured reflect the half-life of individual proteins in the total synaptic pool.

Importantly, all of the proteins whose turnover was accelerated by activity (Bicuc, **Fig. 4b**) were decreased in the PSD fractions from highly active cultures (**Fig. 2b**, right panel). On the other hand, the proteins whose rate of loss from synaptosomal fractions was unchanged by activity (**Fig. 4c**) remained as a larger mole fraction of the total protein in synaptically active PSDs (**Fig. 2b**, right panel). The latter effect could have resulted from activity-dependent recruitment or trafficking to the synapse[10] or from the accelerated loss of neighboring proteins in the PSD leav-

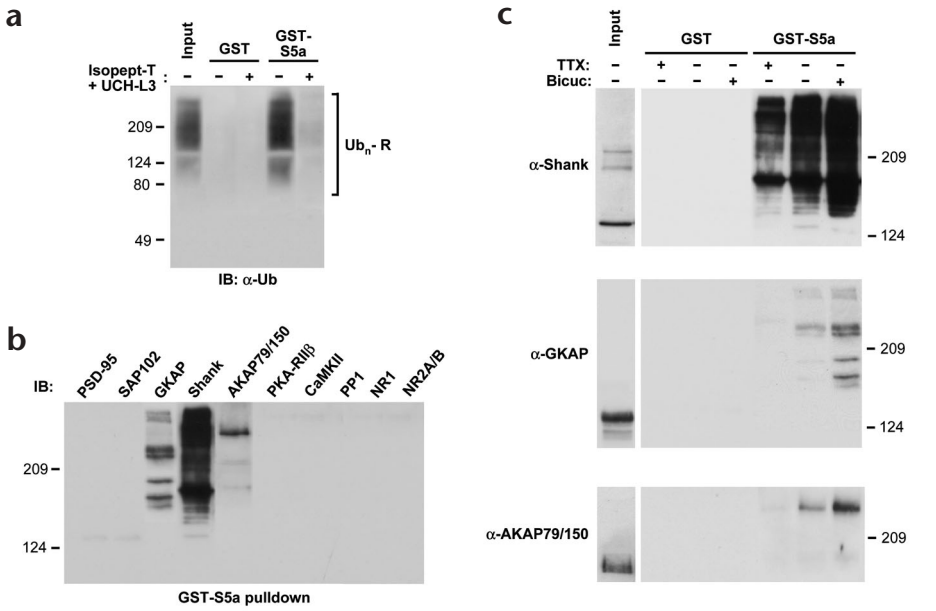

Fig. 6. Activity regulates ubiquitination of the postsynaptic scaffolds Shank, GKAP and AKAP79/150. (**a**) GST pull-down assays for polyubiquitinated proteins were performed on denatured cortical neuron synaptosomal membranes pretreated in the presence (+) or absence (–) of the deubiquitinating enzymes isopeptidase-T (Isopept-T) and UCH-L3 (5 μg each, 60 min, RT) using either GST alone or GST fusions of the polyubiquitin-binding proteasome subunit S5a (GST-S5a). Eluted proteins were assayed for ubiquitin conjugates by anti-ubiquitin (Ub) immunoblot (IB). Molecular mass markers in kDa are shown. (**b**) Poly-ubiquitinated proteins purified from denatured cortical neuron synaptosomal membranes were probed for the presence of the indicated PSD proteins. (**c**) Poly-ubiquitinated proteins were isolated from synaptically inhibited (+TTX, –Bicuc) and synaptically activated (–TTX, +Bicuc) cortical neuron synaptosomal membranes using GST-S5a pulldown and probed for the presence of Shank, GKAP and AKAP79/150. Note that, as expected, Shank, GKAP and AKAP79/150 were present as higher molecular mass species in the polyubiquitin precipitates compared to the total synapotosomal membrane fraction (input) and were not precipitated by GST alone.

ing unaffected proteins (NR2A, mGluR1, PSD-95, Homer and CaMKII) in relative molar excess (**Fig. 4c**). Consistent with the latter notion, overall PSD mass yield was reduced in active cortical cultures relative to inactive cultures (Bicuc, 1.4 ± 0.3 μg PSD protein per mg of total cortical neuron protein; TTX, 2.4 ± 0.5 μg PSD protein per mg; $n = 13$ preps, $P < 0.05$, t-test) despite no change in the number or survival of neurons (data not shown) or the number of synapses (**Fig. 3**), suggesting an accompanying change in PSD size[5]. Together, these results show that activity regulates the half-life of proteins at the synapse and provide strong evidence that such regulated turnover is a primary determinant of postsynaptic composition.

Activity-dependent ubiquitin conjugation in the PSD

Because the turnover of many cellular proteins occurs via covalent attachment of ubiquitin and subsequent degradation by the proteasome[19], I next examined whether synaptic activity regulates ubiquitin conjugation of PSD proteins. Under control conditions, ubiquitin conjugates were abundant in PSD fractions isolated from cortical neurons (**Fig. 5a**) and brain (data not shown). Remarkably, the level of ubiquitin conjugates in the PSD decreased ~50% upon synaptic blockade (51.8 ± 12.2% relative to control, $P < 0.01$; 2 μM TTX, 48 h) and increased twofold in synaptically active PSDs (200 ± 11.4% relative to control, $P < 0.01$; 40 μM Bic, 48 h) (**Fig. 5a** and **b**). This effect was reversible by drug washout (**Fig. 5a** and **b**) (TTX washout, 99.4 ± 8.2% relative to control; Bic washout, 110 ± 11.7% relative to control), required glutamate receptor activation (data not shown) and was not due to alterations in either 20S proteasome expression level or proteasome enzymatic activity (**Fig. 5c**). Thus, these findings support activity-dependent ubiquitin conjugation of PSD proteins.

To directly test for *de novo* ubiquitin conjugation at synapses, *in vitro* ubiquitination assays were performed on cytosol or synaptosome fractions from rat brain (3–4 week old) with subsequent purification of PSDs from the synaptosomes (**Fig. 5d**). Using this approach, robust ATP-dependent ubiquitin conjugation was observed in cytosol as well as synaptosome and PSD fractions (**Fig. 5d**), indicating that biochemically enriched synaptic fractions possess all of the necessary enzymatic machinery and relevant substrates for ubiquitin incorporation. To test whether activity regulates ubiquitin conjugation at the synapse, similar assays were performed on subcellular fractions from control, synaptically active and synaptically inhibited cortical neurons. Consistent with the regulated abundance of ubiquitinated PSD proteins (**Fig. 5a** and **b**), ubiquitin conjugation in synaptosomes and the PSD was markedly reduced after chronic activity blockade (synaptosomes, 44.8 ± 7.6% relative to control; PSD, 29.7 ± 18.2% relative to control, $P < 0.001$; 2 μM TTX, 48 h) and augmented upon excitatory synaptic activation (synaptosomes, 148 ± 14% relative to control; PSD, 207 ± 11.7% relative to control; $P < 0.001$; 40 μM bicuculline, 48 h) (**Fig. 5e** and **f**). In contrast, ubiquitin conjugation in cytosol fractions was unaltered by activity (TTX, 86.7 ± 7.4% relative to control; Bicuc, 92.0 ± 10.9% relative to control) (**Fig. 5e** and **f**), providing direct evidence for selective activity-dependent control over ubiquitin conjugation at the synapse. Indeed, the effect of activity on ubiquitin conjugation was even more pronounced among PSD proteins than synaptosome proteins as a whole (**Fig. 5e** and **f**), indicating that the bulk of ubiquitin conjugation occurred in postsynaptic compartments. These results support the protein turnover data obtained in **Fig. 4a** and suggest that a significant portion of PSD turnover is due to the targeting of postsynaptic proteins for degradation by the ubiquitin-proteasome system.

Ubiquitination of postsynaptic scaffolds

To identify postsynaptic substrates for ubiquitin conjugation, polyubiquitinated proteins were purified from cortical neuron synaptosomal membranes using immobilized fusion proteins of the high-affinity polyubiquitin binding proteasome subunit S5a (ref. 35). As above (**Fig. 5**), ubiquitinated proteins were abun-

© 2003 Nature Publishing Group http://www.nature.com/natureneuroscience

© 2003 Nature Publishing Group http://www.nature.com/natureneuroscience

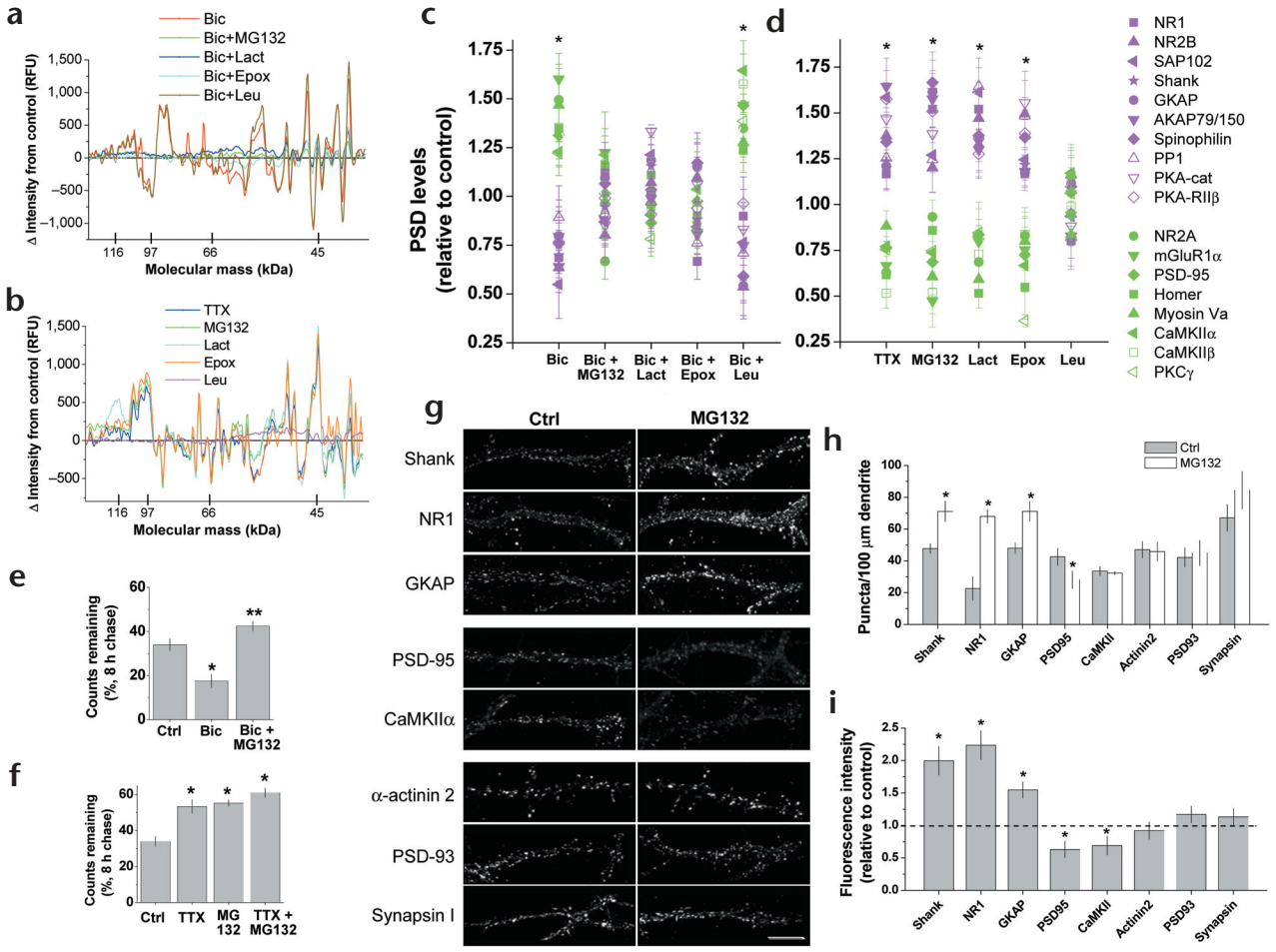

Fig. 7. Activity-dependent remodeling of the PSD results from ubiquitin-proteasome–mediated degradation. (**a**) Absolute changes in protein signal intensity in PSD fractions from synaptically active (Bic) cortical neurons in the presence or absence of the proteasome inhibitors MG132 (10 μM, 24 h), lactacystin (Lact, 1 μM, 24 h) or epoxomicin (Epox, 5 μM, 24 h), or the lysosome inhibitor leupeptin (25 μg/ml, 24 h), relative to control. (**b**) Absolute changes in protein signal intensity in PSD fractions from TTX-, MG132-, lactacystin (Lact)-, epoxomicin (Epox)- or leupeptin (Leu)-treated cortical neurons relative to control. (**c**) Quantitative immunoblot analysis of selected PSD proteins 24 h after adding bicuculline (Bic) in the presence or absence of proteasome inhibitors (MG132, lactacystin or epoxomicin) or lysosome inhibitors (leupeptin) ($n = 4$ for each time point). *$P < 0.0001$ between the complete sets of green and magenta proteins, ANOVA. See also **Supplementary Table 2**. (**d**) Quantitative immunoblot analysis of selected PSD proteins 24 h after adding TTX, MG132, lactacystin (Lact), epoxomicin (Epox) or leupeptin (Leu) as above ($n = 4$ for each time point). Statistics as in (**c**). See also **Supplementary Table 2**. (**e**) Percentage of remaining ^{35}S-labeled protein from control, bicuculline-, and bicuculline/MG132-treated cortical neuron PSDs 8 h after a 4 h pulse (*$P < 0.01$ relative to control; ** $P < 0.01$ relative to control, $P < 0.001$ relative to Bic alone; $n = 6$, t-test). (**f**) Percentage of remaining ^{35}S-label protein from control, TTX-, MG132- and TTX + MG132–treated cortical neuron PSDs 8 h after a 4 h pulse (*$P < 0.01$ relative to control, $n = 6$, t-test). (**g**) Proteasome-mediated degradation controls the accumulation or reduction of PSD proteins at synaptic sites. Cultured hippocampal neurons (24–30 d.i.v.) were treated with either 10 μM MG132 or control solution for 24 h before fixation, permeabilization and staining for synaptic proteins. Scale bar, 10 μm. (**h**,**i**) Quantitative analysis showed changes in the number of PSD protein puncta per 100 μm dendrite (**h**) and in synaptic fluorescence intensity (**i**) after MG132 treatment, consistent with the biochemical data of (**b**) and (**c**). Note that the overall number of synapses revealed by synapsin staining was unchanged. Data represent means ± s.e.m. from 20 neurons for each condition. *$P < 0.01$ relative to control, t-test.

dant in synaptosomal membranes (**Fig. 6a**, left lane), and these proteins could be readily isolated by pulldown assays on denatured synaptosomal membranes using GST-S5a (**Fig. 6a**, lane 4). Pretreatment of synaptosomal membranes with the de-ubiquitinating enzymes isopeptidase-T and ubiquitin C-terminal hydrolase L3 (UCH-L3) abolished binding to S5a (**Fig. 6a**, lane 5), and no detectable polyubiquitinated proteins were bound by GST alone (**Fig. 6a**, lanes 2 and 3), indicating the specificity of the affinity isolation. Immunoblot analysis of isolated polyubiquitinated proteins using a panel of antibodies against PSD proteins revealed the presence of high molecular weight ubiquitinated species for three multivalent postsynaptic scaffolds[4,32,36]: Shank, GKAP and AKAP79/150 (**Fig. 6b**). In contrast, several other PSD proteins, including PSD-95, SAP102, PKA-RIIβ, CaMKII, PP1, NR1 and NR2A/B, were not present in GST-S5a pulldowns (**Fig. 6b**). Interestingly, each of the three ubiquitinated proteins—Shank, GKAP and AKAP79/150—are decreased in abundance at active synapses (**Fig. 2** and **3**), conditions under which ubiquitin conjugation of postsynaptic proteins is enhanced (**Fig. 5**).

To directly test whether activity regulates ubiquitination of Shank, GKAP and AKAP79/150, GST-S5a pulldowns were performed on denatured synaptosomal membrane fractions from cortical neurons

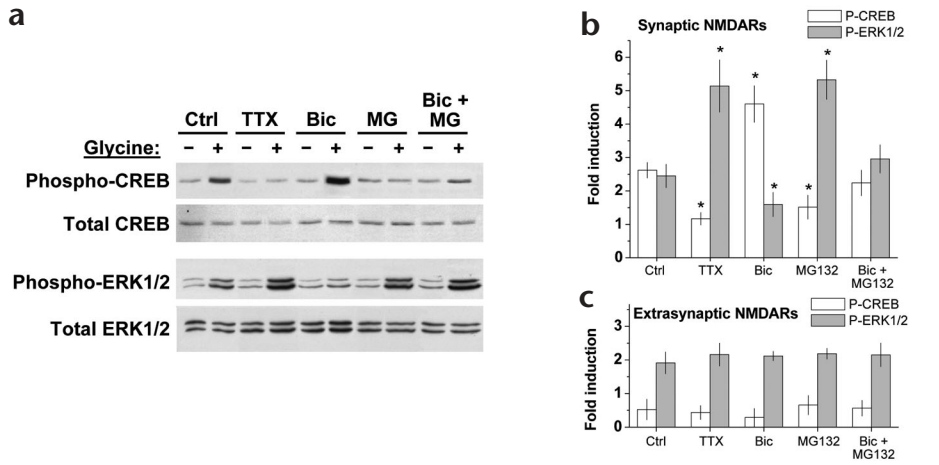

Fig. 8. Activity level and proteasome-mediated degradation regulate synaptic signaling. (**a**) Activity and proteasome function enhance the coupling of synaptic NMDA receptors to CREB and reduce coupling to ERK. Cortical neurons (21–24 d.i.v.) were pretreated for 24–48 h with control solution, TTX (2 μM), bicuculline (Bic, 40 μM), MG132 (MG, 10 μM) or bicuculline plus MG132. The phosphorylation of CREB and ERK was then assayed before (–) and after (+) stimulation of synaptic NMDA receptors with glycine (200 μM, 15 min) as indicated (see Methods for details). Blots were stripped and reprobed for total CREB and total ERK (Methods). (**b**) The fold induction of CREB and ERK1/2 phosphorylation by synaptic NMDA receptor activation was quantified by measuring phosphorylated/total protein band intensity ratios of glycine-stimulated cultures and normalizing to values obtained from sister cultures not treated with glycine as in (**a**). Data represent means ± s.e.m. ($n = 6$, $^*P < 0.05$ relative to the fold induction observed in control cultures, *t*-test). (**c**) Chronic changes in activity and proteasome inhibitors do not affect signaling via extrasynaptic NMDA receptors. Cortical neurons were pretreated as in (**a**), and CREB and ERK1/2 phosphorylation was quantified as in (**b**) after selective activation of extrasynaptic NMDARs using a synaptic NMDAR blocking technique (Methods). (**d**) Hippocampal neurons (24–30 d.i.v.) were pretreated with control solution, TTX, bicuculline or MG132 as in (**a**) before incubation with (Glycine stim.) or without (Unstim.) 200 μM glycine. Cells were fixed, permeabilized and stained for phosphorylated CREB (P-CREB) or phosphorylated ERK1/2 (P-ERK1/2). Scale bar, 20 μm.

© 2003 Nature Publishing Group http://www.nature.com/natureneuroscience

treated with TTX, bicuculline or control solution. Blockade of synaptic activity with TTX resulted in a marked reduction in the ubiquitination of all three synaptic scaffolds (**Fig. 6c**). Conversely, increasing excitatory synaptic activity profoundly enhanced their ubiquitin conjugation (**Fig. 6c**). These data are consistent with the activity-dependent regulation of *de novo* ubiquitin conjugation (**Fig. 5**) and, furthermore, indicate that ubiquitin conjugation is selective and specific for a subset of PSD proteins. Indeed, despite the fact that NR2B, SAP102, PP1 and PKA-RIIβ are all reduced in abundance in active PSDs (**Fig. 2**), none of these proteins showed detectable polyubiquitination (**Fig. 6b**), suggesting that ubiquitin-dependent degradation of Shank, GKAP and AKAP79/150 may control the stability and abundance of additional PSD proteins which themselves are not targeted by ubiquitin.

PSD reorganization by the ubiquitin-proteasome system

If ubiquitin conjugation (**Figs. 5** and **6**) and protein turnover (**Fig. 4**) via the proteasome ultimately lead to the observed global changes in PSD molecular composition (**Figs. 1–3**), then blocking proteasome-mediated degradation should (i) decrease PSD turnover, thereby producing a protein profile that mimics the synaptically inactive state and (ii) prevent activity-induced remodeling. Consistent with (ii), treatment of cortical neurons with any of three structurally distinct proteasome inhibitors—MG132, lactacystin or epoxomicin—prevented the characteristic changes in PSD protein intensity profiles caused by elevating synaptic activity with bicuculline (**Fig. 7a**). Furthermore, the segregation of specific proteins into groups which accumulate or diminish in synaptically active PSDs (40 μM bicuculline, 24 h) was likewise blocked by proteasome inhibition (**Fig. 7c** and **Supplementary Table 2** online). This effect was selective for proteasome-mediated degradation, as inhibition of the lysosome with leupeptin had no effect on activity-induced molecular remodeling (**Fig. 7a** and **c**, last column; **Supplementary Table 2**). Importantly, inhibiting the proteasome prevented the activity-induced increase in total PSD protein turnover (**Fig. 7e**) (percentage of ^{35}S-labeled protein remaining after 8 h chase: Ctrl, 34.0 ± 5.5%; Bic, 17.5 ± 6.1%; Bic + MG132, 42.4 ± 4.6%; $P < 0.01$) and did not itself reduce synaptic activity measured by mEPSC amplitudes and frequencies (T. Otsuka and M.D.E., unpub. observ.).

In contrast to the effect on activated PSDs, treatment of cortical neurons with proteasome inhibitors in the absence of bicuculline mimicked the effect of synaptic blockade. Specifically, PSD protein intensity profiles of neurons treated with each of three distinct proteasome inhibitors were nearly identical to those from TTX-treated neurons (**Fig. 7b**). In addition, all proteins that accumulated or dwindled in the PSD upon synaptic blockade (2 μM TTX, 24 h) did so to nearly the same extent when the proteasome was inhibited (**Fig. 7d**). In each case, inhibition of lysosomal degradation had no significant effect on PSD protein intensity profiles (**Fig. 7b**) or molecular composition (**Fig. 7d** and **Supplementary Table 2**). Moreover, proteasome inhibitors

© 2003 Nature Publishing Group http://www.nature.com/natureneuroscience

slowed total PSD protein turnover to the same degree as synaptic blockade, and these effects occluded one another (**Fig. 7f**), suggesting that activity- and proteasome-mediated remodeling occur via the same mechanism.

To determine whether proteasome-dependent compositional changes in the PSD occurred globally or were restricted to a subset of synapses, immunofluorescent staining for PSD proteins was performed on hippocampal neurons after treatment with MG132 (**Fig. 7g**). Consistent with the biochemical results (**Fig. 7c** and **d**), both the number and staining intensity of Shank, NR1 and GKAP immunoreactive clusters were dramatically increased, whereas synaptic staining for PSD-95 and CaMKIIα was slightly decreased; no quantitative changes were observed in staining for α-actinin2 or PSD-93 (**Fig. 7h** and **i**). In all cases, punctate clusters of PSD proteins colocalized with synapsin I (data not shown). Importantly, all neurons examined showed similar changes in synaptic staining ($n = 20$ for each condition) with no detectable differences between synapses on individual neurons (**Fig. 7g** and data not shown). In addition, MG132 had no effect on the number of synapses detected by synapsin I staining under the experimental conditions (**Fig. 7h** and **i**). Together with the biochemical experiments above, these findings indicate that proteasome-mediated degradation controls activity-dependent protein turnover and global compositional changes in the PSD.

Activity alters signaling via CREB and ERK

In response to chronic alterations of excitatory synaptic activity, the electrical properties of synaptic transmission change in a homeostatic fashion[13,30,34]. To test whether additional aspects of synaptic signaling are regulated by the activity state of the synapse, I examined the ability of NMDA receptors to activate CREB and ERK-MAPK—two prominent signal transduction cascades organized by the PSD and involved in synaptic plasticity[3,18,37]. Synaptic NMDA receptors were selectively activated using a previously described glycine application method[38], and the phosphorylation state of CREB and ERK-MAPK was measured 15 minutes later using phosphorylation state-specific antibodies. As expected[39,40], activation of synaptic NMDA receptors under control conditions produced a two- to three-fold increase in phosphorylation of CREB at serine 133 (top panel, lanes 1 and 2 in **Fig. 8a**; also **Fig. 8b** and **d**) and a similar magnitude increase in dual phosphorylation of p44/42 MAPK (ERK1/2) at threonine 202 and tyrosine 204 (third panel, lanes 1 and 2 in **Fig. 8a**; also **Fig. 8b** and **d**), reflecting the respective activation of these proteins[18,37]. Upon chronic activity blockade (TTX), glycine application produced a dramatically enhanced degree of ERK-MAPK phosphorylation (5.1 ± 0.8 fold increase in phospho-ERK1/2 compared to 2.5 ± 0.3 fold in control neurons), whereas the coupling of synaptic NMDA receptors to CREB was almost completely abolished (1.2 ± 0.2 fold increase in phospho-CREB compared to 2.6 ± 0.2 fold in control neurons) (**Fig. 8a**, **b** and **d**). The bidirectional effect on NMDA receptor–dependent signaling via these two pathways indicates that changes were not simply due to altered numbers of synaptic NMDA receptors in active and inactive cultures[12,30]. Moreover, in synaptically active cultures (40 μM bicuculline), this pattern of downstream signaling was reversed. Specifically, NMDA receptor–dependent phosphorylation of ERK-MAPK was reduced (1.6 ± 0.8 fold increase in phospho-ERK1/2 compared to 2.5 ± 0.3 fold in control neurons), whereas phosphorylation of CREB was enhanced (4.6 ± 0.5 fold increase in phospho-CREB compared to 2.6 ± 0.2 fold in control neurons) (**Fig. 8a**, **b** and **d**). Importantly, the observed activity-dependent changes in signaling to CREB and ERK-MAPK were due to synaptic modifications, as selective activation of extrasynaptic receptors using a synaptic block pharmacological approach[41] (see Methods for details) caused a characteristic dephosphorylation of CREB[40,42] and an increased phosphorylation of ERK-MAPK (**Fig. 8c**, Ctrl) that remained unchanged by prolonged increases (bicuculline) or decreases (TTX) in excitatory synaptic activity (**Fig. 8c**).

To test whether activity-dependent alterations in synaptic signaling to CREB and ERK-MAPK could be explained by proteasome-dependent remodeling of postsynaptic signaling complexes (**Fig. 7**), I pretreated cortical neurons with proteasome inhibitors before stimulating synaptic NMDA receptors with glycine. Much like synaptic blockade, proteasome inhibition augmented synaptic NMDA receptor-dependent activation of ERK-MAPK (MG132, 5.3 ± 0.6 fold increase; Ctrl, 2.5 ± 0.3) and nearly eliminated glycine-induced activation of CREB (MG132, 1.5 ± 0.4 fold increase; Ctrl, 2.6 ± 0.2) (**Fig. 8a**, **b** and **d**). Moreover, treatment of cortical neurons with MG132 prevented both the activity-dependent increase in glycine-stimulated CREB phosphorylation (Bic + MG132, 2.2 ± 0.4 fold increase compared to 4.6 ± 0.5 for Bic alone and 2.6 ± 0.2 for control) and the activity-dependent decrease in NMDA receptor–stimulated ERK-MAPK phosphorylation (Bic + MG132, 3.0 ± 0.4 fold increase compared to 1.6 ± 0.4 for Bic alone and 2.4 ± 0.3 for control) (**Fig. 8a** and **b**). Together, these data indicate that activity level bidirectionally and reciprocally regulates synaptic signaling to CREB and ERK-MAPK and are consistent with results presented above, indicating a role for activity in the global reorganization of postsynaptic signaling complexes. Finally, these results provide further evidence indicating that the functional and molecular organization of the postsynaptic membrane is regulated by activity-dependent protein turnover through the ubiquitin-proteasome system.

Discussion

In the present study, I have shown that long-lasting changes in synaptic activity cause pervasive reorganization of the postsynaptic density at cortical neuron synapses. In response to increased activity, postsynaptic proteins, including specific postsynaptic scaffolds, become highly ubiquitinated, and the turnover of a subset of PSD proteins is enhanced. This destabilization and increased turnover of PSD proteins in turn leads to loss of specific multiprotein modules, which reversibly alters the global molecular character and signaling properties of the postsynaptic membrane. In contrast, activity deprivation reduces ubiquitin conjugation and proteasome-mediated turnover, thereby producing reciprocal changes in PSD composition and synaptic signaling.

These results provide a quantitative demonstration of dynamic multiprotein changes in the postsynaptic membrane in response to synaptic activity. I examined nearly 30 PSD constituents and measured their relative stoichiometric abundance over time in response to activity. Changes in PSD composition are bidirectional, saturable, reversible and involve multiple classes of PSD proteins[3,4], suggesting important roles in the electrical, structural and signaling properties of the synapse[2,11]. For example, activated PSDs are enriched in CaMKII, whereas inactive synapses contain abundant PP1, a reciprocal arrangement mirrored by the opposing effects of these signaling enzymes on synaptic efficacy. Surprisingly, the time course and magnitude of bidirectional change in PSD composition was remarkably similar across all protein classes. The striking resemblance among the patterns of protein accumulation and loss from the PSD suggests

© 2003 Nature Publishing Group http://www.nature.com/natureneuroscience

that large sets of postsynaptic proteins exist as functional or physical ensembles. This resemblance also implies that control over PSD composition may be governed by the incorporation or removal of certain key 'master organizing molecules' that preserve stoichiometric relationships between PSD proteins.

Results here further indicate that protein removal mechanisms regulate the molecular architecture of synapses and specifically identify ubiquitin conjugation and proteasome-mediated degradation as a primary mechanism for activity-dependent remodeling of the PSD. Consistent with this idea, ubiquitin-processing enzymes can regulate synaptic transmission[23,24], long-term potentiation[22], facilitation[21] and synapse development[25,27]. Here I have shown that activity regulates *de novo* ubiquitin conjugation and turnover of postsynaptic proteins generally, and ubiquitination of certain scaffolding molecules specifically. Activity-dependent ubiquitination of postsynaptic proteins may thus provide a common regulatory mechanism linking rapid receptor trafficking and degradation[31] to dynamic changes in PSD structure and morphology[2] that alter synapse strength[21–23]. Indeed, turnover of postsynaptic receptors[13,31,43] and protein kinases[44] contributes to plastic change at vertebrate and invertebrate synapses. Importantly, the results presented here do not exclude a role for gene transcription and protein synthesis in regulating PSD composition or molecular reorganization. Indeed, much like the remodeling of growth cones[45], both synthesis and degradation almost certainly contribute (M.D.E., unpub. observ.)[16–18,37]. Rather, the current findings indicate that activity-dependent protein turnover joins stimulus-dependent gene expression and protein synthesis[16,17] in engineering durable changes in the cellular machinery that govern synaptic morphology and function.

The modular multiprotein nature of activity-dependent durable changes may be due to regulated removal or turnover of 'master organizing molecules'. Indeed, here I have shown that the postsynaptic scaffolds Shank, GKAP and AKAP79/150 undergo selective activity-dependent ubiquitination. Shank and GKAP are multivalent adaptors that bind to each other and to numerous additional proteins in the PSD[4,32]. In addition, AKAP79/150 anchors PKA and PP2B to complexes containing glutamate receptors and PSD-95 family members[36]. The ubiquitin-dependent removal of one or more of these scaffolds could provide a mechanism for selectively destabilizing numerous associated proteins in the PSD complex, thereby accounting for the 'clusters' of proteins coregulated by activity.

Measurements of synaptic half-life in the current study reflect both degradation and permanent transport out of synapses. Such transport represents an essentially permanent trafficking event that does not reverse over a period of ~48 hours—quite different from the rapid recycling of AMPA receptors[31,46] and the rapidly reversible translocation of NMDARs and CaMKII[47] at synapses. However, turnover and trafficking of different PSD proteins may be functionally linked. For example, CaMKII and PSD-95 accumulated at active synapses without a change in turnover rate. Nonetheless, the long-term activity-dependent increases of CaMKII, PSD-95 and other proteins in the PSD requires proteasome-mediated degradation. In such cases, synaptic accumulation may require degradation of a blocking or space-occupying protein in the postsynaptic density, or degradation of an inhibitory chaperone that sequesters proteins away from the PSD, which then allows for translocation to the synapse. It is important to note that differences in neuronal subtypes examined (cortical versus hippocampal) and methods for measuring synapse incorporation (presence in PSD fraction versus immunocytochemical detection at synapse) may also produce differences in measured synaptic levels of specific PSD proteins (for example, CaMKIIα versus CaMKIIβ)[15]. Given such possibilities, it will be important for future studies to delineate the mechanisms by which ubiquitin conjugation and proteasomal degradation contribute to synaptic accumulation or loss for each individual PSD protein.

Results presented here further show that chronic alterations in activity alter downstream signaling to CREB and ERK-MAPK. Synaptic signaling from NMDA receptors to CREB activates gene transcription that is critical for diverse neuronal functions, most prominently plasticity, learning and memory[37]. Likewise, NMDA receptor–dependent signaling to ERK-MAPK triggers both local and nuclear signaling events that are important for controlling dendritic morphology, neuronal excitability, synaptic potentiation and memory formation[18]. Interestingly, although both pathways can be activated by NMDA receptors, they can be functionally uncoupled by development[42], by selective activation of extrasynaptic versus synaptic NMDA receptors[40] and by the pattern and spatial features of local Ca^{2+} signaling[39]. As a consequence, selective activation of CREB and ERK-MAPK produces specific plasticity and functional responses[18,37,40,48,49]. The coupling of synaptic NMDA receptors to CREB and ERK-MAPK involves a diverse set of proteins organized in the PSD[3,4]. Here I have shown reciprocal regulation of CREB and ERK-MAPK pathways in response to prolonged alterations in synaptic activity associated with PSD remodeling. In particular, NMDA receptors at active synapses elicited greater activation of CREB, whereas their counterparts at inactive synapses were selectively coupled to ERK-MAPK. These results expand the range of functional synaptic changes associated with homeostatic plasticity beyond the electrical properties of the synapse and provide strong evidence that activity-dependent reorganization of the postsynaptic apparatus regulates multiple facets of synaptic signaling.

METHODS

Antibodies. Antibodies used in these experiments are described in **Supplementary Methods** online.

Primary neuron cultures. High-density cortical neurons and low-density hippocampal neurons were prepared from E18 rat embryos and maintained for 14–30 d *in vitro* as described[31]. Neurons were either kept in control medium or treated with tetrodotoxin (2 μM), bicuculline (40 μM), D-AP5 (50 μM), CNQX (10 μM), MG132 (1, 10 or 50 μM), lactacystin (10 μM) and/or epoxomicin (5–10 μM) for 2–72 h as indicated.

Synaptosome and PSD purifications. Cytosol, synaptosome, synaptosomal membrane and PSD fractions from rat brain were purified essentially as described[29]. Cytosol, synaptosome, synaptosomal membrane and PSD fractions from cultured cortical neurons were prepared using a small-scale modification of this procedure.

Protein profiling and quantification. PSD fractions (1–2 μg) were separated by SDS-PAGE and visualized by staining fixed gels with Sypro Ruby (Molecular Probes, Eugene, Oregon). Stained gels were scanned on a fluorescent imager (Storm 860, Amersham Biosciences, Piscataway, New Jersey), and regions of the one-dimensional gel were subjected to linescan analysis using ImageQuant 5.0 software.

Immunoblot analysis of PSD proteins. PSD fractions (1–2 μg) were resolved by SDS-PAGE and transferred to a polyvinylidene fluoride (PVDF) membrane, and proteins of interest were detected by immunblot (ECL Plus, Amersham). Quantification of band intensity was performed on a phosphorimager (Storm 860, Amersham Biosciences) using ImageQuant 5.0 software.

© 2003 Nature Publishing Group http://www.nature.com/natureneuroscience

Quantitative immunofluorescence microscopy. Hippocampal neurons were processed as described[31]. Wide-field epifluorescence images were acquired on a Nikon TE300 inverted microscope. Confocal images were obtained using a Yokogawa spinning disk confocal (Solamere Technology Group, Salt Lake City, Utah). Images were acquired and analyzed using Metamorph (Universal Imaging Corporation, Downingtown, Pennsylvania) with a 12-bit cooled CCD camera (Hamamatsu Inc., Bridgewater, New Jersey). PSD protein puncta were quantified as described[31].

^{35}S pulse-chase labeling and immunoprecipitation. Metabolic labeling of cortical neurons treated for 12 h with either control solution, TTX (2 μM) or bicuculline (40 μM) was performed as described[50], except that labeling was done with a 2.0 mCi per 60 mm dish of ^{35}S-cysteine/methionine (Express Protein Labeling Mix, Perkin Elmer Life Sciences, Boston, Massachussetts) for 12 h at 37 °C, and chase times in normal media were 0, 4, 8, 24 and 48 h. For determination of total ^{35}S incorporation, an equal amount of PSD protein was either subjected to scintillation counting (LS6500, Beckman Coulter Inc., Fullerton, California) or resolved by SDS-PAGE, and total ^{35}S-labeled protein was detected and quantified on a phosphorimager (Storm 860, Amersham Biosciences). For measuring the turnover of individual proteins, synaptosomes from labeled cortical neurons were subjected to immunoprecipitation with indicated antibodies. Immunoprecipitates were resolved by SDS-PAGE, and precipitated ^{35}S-labeled proteins were detected and quantified on a phosphorimager. Protein turnover was measured as the fractional decrease in ^{35}S-labeled protein over time, normalized to the amount of ^{35}S-labeled protein present at time zero. Time constants for protein turnover (τ) were determined by fitting the data to a single exponential function of the form $y = y_o + Ae^{-t/\tau}$ where y_o and A are constants.

Proteasome activity assays. Cortical neuron lysates (100 μg) were incubated in proteolysis buffer (10 mM HEPES, pH 7.4, 5 mM ATP, 0.5 mM DTT, 5 mM $MgCl_2$) in the presence or absence of proteasome inhibitors (50 μM MG132 or 10 μM lactacystin) for 10 min at 37 °C before the addition of 100 μM of the fluorogenic proteasome peptide substrate Suc-LLVY-AMC (Calbiochem, San Diego, California) in a 96-well microtiter plate. Fluorescence (380 nm excitation, 460 nm emission) was monitored on a microplate fluorometer (FluoStar, BMG Labtechnologies, Durham, North Carolina) every 5 min for 2 h.

Ubiquitin conjugation assays. Cytosol or synaptosome fractions (100 μg) were added to an equal volume of 2× ubiquitin conjugation buffer (100 mM Tris, pH 7.8, 10 mM $MgCl_2$, 1 mM DTT, 150 μM MG132, 4 μM ubiquitin aldehyde, 5 mM AMP-PNP, 20 mM ATP, 20 mM creatine phosphate, 0.5 mg/ml creatine phosphokinase). After a 5-min preincubation at 37 °C, samples were incubated in the presence or absence of GST-ubiquitin (10 μg) for 60 min at 37 °C with occasional mixing. Samples were then either immediately solubilized in SDS-PAGE sample buffer, or PSD fractions were purified from synaptosomes as described above before solubilizing in SDS-PAGE sample buffer. GST-ubiquitin–conjugated proteins were then resolved by SDS-PAGE, transferred to PVDF membrane and detected by immunoblot analysis with anti-GST.

GST pulldowns of polyubiquitinated proteins. Synaptosomal membrane fractions were prepared from cortical neurons incubated for 12 h in control solution, TTX or bicuculline (as above) and for 4 h in 50 μM MG132. For de-ubiquitination controls, membranes (200 μg) were resuspended in 25 mM HEPES, pH 7.4 and 10 mM DTT and incubated with 5 μg each of isopeptidase-T (Calbiochem) and UCH-L3 (Affiniti Research, Exeter, UK) for 60 min at RT. All samples were solubilized and denatured in TBS containing 0.2% SDS (10 min, 70 °C), diluted into 1% Triton X-100 and 5% glycerol and kept in 1 μM ubiquitin aldehyde (Calbiochem) and 50 μM MG132 throughout. Binding was performed with GST-agarose or GST-S5a agarose (Affiniti Research) for 2 h at 4 °C. Bound proteins were washed extensively in TBS + 1% Triton + 5% glycerol and eluted by boiling in SDS-PAGE sample buffer before SDS-PAGE, then transferred to the PVDF membrane and detected by immublot analysis with appropriate antibodies.

NMDAR-dependent activation of CREB and ERK. Neurons were pretreated with control solution, TTX, bicuculline and/or MG132 as above. Biochemical experiments were performed on cortical neurons in 60 mm dishes (2–3 × 10^6 cells/dish), and immunostaining experiments were performed on hippocampal neurons grown on glass coverslips in 12-well dishes (50,000 cells/well). Synaptic NMDARs were selectively activated by application of glycine (200 μM) in bath solution lacking Mg^{2+} (140 mM NaCl, 1.3 mM $CaCl_2$, 10 mM KCl, 25 mM HEPES pH 7.4, 33 mM glucose, 0.5 μM TTX, 1 μM strychnine, 20 μM bicuculline) as previously described[38], except that cells were exposed for 15 min. For activation of extrasynaptic receptors, I used a synaptic blockade approach[41]. Neurons were transferred to bath solution containing 20 μM MK-801, 10 μM nifedipine and 50 μM MCPG and synaptic glutamate release stimulated by depolarizing the cells with 50 mM KCl. Activated synaptic NMDA receptors are rapidly blocked under these conditions by the essentially irreversible open channel blocker MK-801 (ref. 41). Neurons were then transferred to media containing 10 μM nifedipine, 40 μM CNQX, 1 μM TTX and 20 μM bicuculline, and unblocked extrasynaptic NMDA receptors were activated with 100 μM NMDA for 15 min. Cells were then either immediately rinsed, scraped into SDS-PAGE sample buffer and processed for immunoblot analysis, or fixed in 4% paraformaldehyde/4% sucrose and processed for immunocytochemistry using CREB, phospho-CREB, ERK1/2 and phospho-ERK1/2 antibodies.

Note: Supplementary information is available on the Nature Neuroscience website.

Acknowledgments

I thank C. Zhang for technical help and J. Hernandez, G. Augustine, T. Blanpied, G. Feng, D. Fitzpatrick, A. Horton, L. Katz, J. McNamara, R. Mooney, Y. Mu, I. Perez-Otano, D. Scott and P. Skene for comments and advice. This work was supported by grants from the NIH (NS39402 and MH64748), McKnight Foundation, Klingenstein Fund, Spinal Cord Research Foundation, NARSAD, Sloan Foundation, Ellison Foundation, Alzheimer's Association and the Muscular Dystrophy Association.

Competing interests statement

The author declares that he has no competing financial interests.

RECEIVED 12 NOVEMBER 2002; ACCEPTED 10 JANUARY 2003

1. Yuste, R. & Bonhoeffer, T. Morphological changes in dendritic spines associated with long-term synaptic plasticity. *Annu. Rev. Neurosci.* **24**, 1071–1089 (2001).
2. Luscher, C., Nicoll, R.A., Malenka, R.C. & Muller, D. Synaptic plasticity and dynamic modulation of the postsynaptic membrane. *Nat. Neurosci.* **3**, 545–550 (2000).
3. Husi, H., Ward, M.A., Choudhary, J.S., Blackstock, W.P. & Grant, S.G. Proteomic analysis of NMDA receptor-adhesion protein signaling complexes. *Nat. Neurosci.* **3**, 661–669 (2000).
4. Sheng, M. & Kim, M.J. Postsynaptic signaling and plasticity mechanisms. *Science* **298**, 776–780 (2002).
5. Murthy, V.N., Schikorski, T., Stevens, C.F. & Zhu, Y. Inactivity produces increases in neurotransmitter release and synapse size. *Neuron* **32**, 673–682 (2001).
6. Geinisman, Y., deToledo-Morrell, L. & Morrell, F. Induction of long-term potentiation is associated with an increase in the number of axospinous synapses with segmented postsynaptic densities. *Brain Res.* **566**, 77–88 (1991).
7. Toni, N., Buchs, P.A., Nikonenko, I., Bron, C.R. & Muller, D. LTP promotes formation of multiple spine synapses between a single axon terminal and a dendrite. *Nature* **402**, 421–425 (1999).
8. Okabe, S., Kim, H.D., Miwa, A., Kuriu, T. & Okado, H. Continual remodeling of postsynaptic density and its regulation by synaptic activity. *Nat. Neurosci.* **2**, 804–811 (1999).
9. Marrs, G.S., Green, S.H. & Dailey, M.E. Rapid formation and remodeling of postsynaptic densities in developing dendrites. *Nat. Neurosci.* **4**, 1006–1013 (2001).
10. Meyer, T. & Shen, K. In and out of the postsynaptic region: signaling proteins on the move. *Trends Cell Biol.* **10**, 238–244 (2000).
11. Turrigiano, G.G. & Nelson, S.B. Hebb and homeostasis in neuronal plasticity. *Curr. Opin. Neurobiol.* **10**, 358–364 (2000).
12. Rao, A. & Craig, A.M. Activity regulates the synaptic localization of the NMDA receptor in hippocampal neurons. *Neuron* **19**, 801–812 (1997).

13. O'Brien, R.J. *et al.* Activity-dependent modulation of synaptic AMPA receptor accumulation. *Neuron* **21**, 1067–1078 (1998).
14. Malinow, R. & Malenka, R.C. AMPA receptor trafficking and synaptic plasticity. *Annu. Rev. Neurosci.* **25**, 103–126 (2002).
15. Thiagarajan, T.C., Piedras-Renteria, E.S. & Tsien, R.W. alpha- and beta-CaMKII: inverse regulation by neuronal activity and opposing effects on synaptic strength. *Neuron* **36**, 1103–1114 (2002).
16. West, A.E. *et al.* Calcium regulation of neuronal gene expression. *Proc. Natl. Acad. Sci. USA* **98**, 11024–11031 (2001).
17. Steward, O. & Schuman, E.M. Protein synthesis at synaptic sites on dendrites. *Annu. Rev. Neurosci.* **24**, 299–325 (2001).
18. Adams, J.P. & Sweatt, J.D. Molecular psychology: roles for the ERK MAP kinase cascade in memory. *Annu. Rev. Pharmacol. Toxicol.* **42**, 135–163 (2002).
19. Glickman, M.H. & Ciechanover, A. The ubiquitin-proteasome proteolytic pathway: destruction for the sake of construction. *Physiol. Rev.* **82**, 373–428 (2002).
20. Hicke, L. Protein regulation by monoubiquitin. *Nat. Rev. Mol. Cell. Biol.* **2**, 195–201 (2001).
21. Hegde, A.N. *et al.* Ubiquitin C-terminal hydrolase is an immediate-early gene essential for long-term facilitation in *Aplysia*. *Cell* **89**, 115–126 (1997).
22. Jiang, Y.H. *et al.* Mutation of the Angelman ubiquitin ligase in mice causes increased cytoplasmic p53 and deficits of contextual learning and long-term potentiation. *Neuron* **21**, 799–811 (1998).
23. DiAntonio, A. *et al.* Ubiquitination-dependent mechanisms regulate synaptic growth and function. *Nature* **412**, 449–452 (2001).
24. Wilson, S.M. *et al.* Synaptic defects in ataxia mice result from a mutation in Usp14, encoding a ubiquitin-specific protease. *Nat. Genet.* **7**, 7 (2002).
25. Murphey, R. & Godenschwege, T. New roles for ubiquitin in the assembly and function of neuronal circuits. *Neuron* **36**, 5 (2002).
26. Hegde, A.N. & DiAntonio, A. Ubiquitin and the synapse. *Nat. Rev. Neurosci.* **3**, 854–861 (2002).
27. Burbea, M., Dreier, L., Dittman, J.S., Grunwald, M.E. & Kaplan, J.M. Ubiquitin and AP180 regulate the abundance of GLR-1 glutamate receptors at postsynaptic elements in *C. elegans*. *Neuron* **35**, 107–120 (2002).
28. Chapman, A.P., Smith, S.J., Rider, C.C. & Beesley, P.W. Multiple ubiquitin conjugates are present in rat brain synaptic membranes and postsynaptic densities. *Neurosci. Lett.* **168**, 238–242 (1994).
29. Cho, K.O., Hunt, C.A. & Kennedy, M.B. The rat brain postsynaptic density fraction contains a homolog of the *Drosophila* discs—large tumor suppressor protein. *Neuron* **9**, 929–942 (1992).
30. Watt, A.J., van Rossum, M.C., MacLeod, K.M., Nelson, S.B. & Turrigiano, G.G. Activity co-regulates quantal AMPA and NMDA currents at neocortical synapses. *Neuron* **26**, 659–670 (2000).
31. Ehlers, M.D. Reinsertion or degradation of AMPA receptors determined by activity-dependent endocytic sorting. *Neuron* **28**, 511–525 (2000).
32. Boeckers, T.M., Bockmann, J., Kreutz, M.R. & Gundelfinger, E.D. ProSAP/Shank proteins—a family of higher order organizing molecules of the postsynaptic density with an emerging role in human neurological disease. *J. Neurochem.* **81**, 903–910 (2002).
33. Liao, D., Zhang, X., O'Brien, R., Ehlers, M.D. & Huganir, R.L. Regulation of morphological postsynaptic silent synapses in developing hippocampal neurons. *Nat. Neurosci.* **2**, 37–43 (1999).
34. Turrigiano, G.G., Leslie, K.R., Desai, N.S., Rutherford, L.C. & Nelson, S.B. Activity-dependent scaling of quantal amplitude in neocortical neurons. *Nature* **391**, 892–896 (1998).
35. Deveraux, Q., Ustrell, V., Pickart, C. & Rechsteiner, M. A 26 S protease subunit that binds ubiquitin conjugates. *J. Biol. Chem.* **269**, 7059–7061 (1994).
36. Michel, J.J. & Scott, J.D. AKAP mediated signal transduction. *Annu. Rev. Pharmacol. Toxicol.* **42**, 235–257 (2002).
37. Lonze, B.E. & Ginty, D.D. Function and regulation of CREB family transcription factors in the nervous system. *Neuron* **35**, 605–623 (2002).
38. Lu, W. *et al.* Activation of synaptic NMDA receptors induces membrane insertion of new AMPA receptors and LTP in cultured hippocampal neurons. *Neuron* **29**, 243–254 (2001).
39. Hardingham, G.E., Arnold, F.J. & Bading, H. A calcium microdomain near NMDA receptors: on switch for ERK-dependent synapse-to-nucleus communication. *Nat. Neurosci.* **4**, 565–566 (2001).
40. Hardingham, G.E., Fukunaga, Y. & Bading, H. Extrasynaptic NMDARs oppose synaptic NMDARs by triggering CREB shut-off and cell death pathways. *Nat. Neurosci.* **5**, 405–414 (2002).
41. Tovar, K.R. & Westbrook, G.L. Mobile NMDA receptors at hippocampal synapses. *Neuron* **34**, 255–264 (2002).
42. Sala, C., Rudolph-Correia, S. & Sheng, M. Developmentally regulated NMDA receptor-dependent dephosphorylation of cAMP response element-binding protein (CREB) in hippocampal neurons. *J. Neurosci.* **20**, 3529–3536 (2000).
43. Akaaboune, M., Culican, S.M., Turney, S.G. & Lichtman, J.W. Rapid and reversible effects of activity on acetylcholine receptor density at the neuromuscular junction *in vivo*. *Science* **286**, 503–507 (1999).
44. Chain, D.G. *et al.* Mechanisms for generating the autonomous cAMP-dependent protein kinase required for long-term facilitation in *Aplysia*. *Neuron* **22**, 147–156 (1999).
45. Campbell, D.S. & Holt, C.E. Chemotropic responses of retinal growth cones mediated by rapid local protein synthesis and degradation. *Neuron* **32**, 1013–1026 (2001).
46. Luscher, C. *et al.* Role of AMPA receptor cycling in synaptic transmission and plasticity. *Neuron* **24**, 649–658 (1999).
47. Fong, D.K., Rao, A., Crump, F.T. & Craig, A.M. Rapid synaptic remodeling by protein kinase C: reciprocal translocation of NMDA receptors and calcium/calmodulin-dependent kinase II. *J. Neurosci.* **22**, 2153–2164 (2002).
48. Minichiello, L. *et al.* Mechanism of TrkB-mediated hippocampal long-term potentiation. *Neuron* **36**, 121 (2002).
49. Wu, G.Y., Deisseroth, K. & Tsien, R.W. Spaced stimuli stabilize MAPK pathway activation and its effects on dendritic morphology. *Nat. Neurosci.* **4**, 151–158 (2001).
50. Mammen, A.L., Huganir, R.L. & O'Brien, R.J. Redistribution and stabilization of cell surface glutamate receptors during synapse formation. *J. Neurosci.* **17**, 7351–7358 (1997).

© 2003 Nature Publishing Group http://www.nature.com/natureneuroscience